oxygen

MDPI

Article

Correlation of the Isotropic NMR Chemical Shift with Oxygen Coordination Distances in Periodic Solids

Jennifer Steinadler, Otto E. O. Zeman † and Thomas Bräuniger *

Department of Chemistry, University of Munich (LMU), Butenandtstr. 5-13, 81377 Munich, Germany; jennifer.steinadler@cup.lmu.de (J.S.); o.e.o.zeman@gmail.com (O.E.O.Z.)
* Correspondence: thomas.braeuniger@cup.lmu.de; Tel.: +49-89-2180-77433
† Current address: Siltronic AG, 84489 Burghausen, Germany.

Abstract: In Nuclear Magnetic Resonance (NMR) spectroscopy, the isotropic chemical shift δ_{iso} is a measure of the electron density around the observed nuclide. For characterization of solid materials and compounds, it is desirable to find correlations between δ_{iso} and structural parameters such as coordination numbers and distances to neighboring atoms. Correlations of good quality are easier to find when the coordination sphere is formed by only one element, as the electron density is obviously strongly dependent on the atomic number. The current study is therefore restricted to nuclides in pure oxygen coordination. It is shown that the isotropic shift δ_{iso} correlates well with the average oxygen distances (as defined by the coordination sphere) for the nuclides ^{23}Na (with spin $I = 3/2$), ^{27}Al ($I = 5/2$), and ^{43}Ca ($I = 7/2$), using literature data for a range of periodic solids. It has been previously suggested for ^{207}Pb ($I = 1/2$) that δ_{iso} may alternatively be related to the shortest oxygen distance in the structure, and our study corroborates this also for the nuclides considered here. While the correlation with the minimal distance is not always better, it has the advantage of being uniquely defined. In contrast, the average distance is strongly dependent on the designation of the oxygen coordination sphere, which may be contentious in some crystal structures.

Keywords: solid-state NMR; ^{23}Na, ^{27}Al, ^{43}Ca chemical shift; oxygen coordination

Citation: Steinadler, J.; Zeman, O.E.O.; Bräuniger, T. Correlation of the Isotropic NMR Chemical Shift with Oxygen Coordination Distances in Periodic Solids. *Oxygen* **2022**, *2*, 327–336. https://doi.org/10.3390/oxygen2030023

Academic Editor: John T. Hancock

Received: 25 July 2022
Accepted: 2 August 2022
Published: 5 August 2022

1. Introduction

Nuclear Magnetic Resonance (NMR) spectroscopy probes the response of the magnetic moments of nuclei in an external magnetic field. Since its inception in 1946 [1], it has developed into a powerful analytical tool, with a wide range of applications in chemistry, physics, and materials science [2–4]. In particular, NMR spectroscopy of inorganic solids has become an established method for the elucidation of structure and dynamics, as a technique complementary to X-ray diffraction (XRD) [4–7]. The successful application of solid-state NMR to crystallographic problems has led to the establishment of a 'Commission on NMR Crystallography and Related Methods' in the International Union of Crystallography [8]. Many crystallographic questions, such as the determination of asymmetric units, or the assignment of space groups may be answered by considering the isotropic chemical shift δ_{iso} of the NMR-observed nuclide in the corresponding structures [5,6]. The chemical shift reflects the modification of the resonance frequency by the electronic charges surrounding the nucleus, which obviously encapsulates information about the coordination sphere, i.e., number and type of neighboring atoms. This three-dimensional electronic shielding is commonly described by a symmetric second-rank tensor. The isotropic chemical shift δ_{iso} is the weighted trace of this tensor:

$$\delta_{iso} = \frac{1}{3}(\delta_{11} + \delta_{22} + \delta_{33}) \quad (1)$$

From solution-state NMR spectra, only δ_{iso} is available. NMR spectra of solids, whether under static or magic-angle spinning conditions [9], may additionally contain information about the individual tensor elements [10–12].

Among other structural information that may be derived from the isotropic chemical shift, one is of particular interest in the context of the current work, namely the attempt to correlate δ_{iso} with interatomic distances between the observed nuclide and the coordinating oxygen atoms. Many inorganic compounds contain oxygen, not just in the form of the O^{2-} ion (as present in oxides) but also in more complex oxyanions such as phosphates PO_4^{3-}, sulphates SO_4^{2-}, carbonates CO_3^{2-}, etc. In many cases, the oxygen atoms form (more or less) regular coordination polyhedra around the elements of the cationic sublattice. Examples for five-, six-, and ninefold coordination by oxygen are depicted in Figure 1.

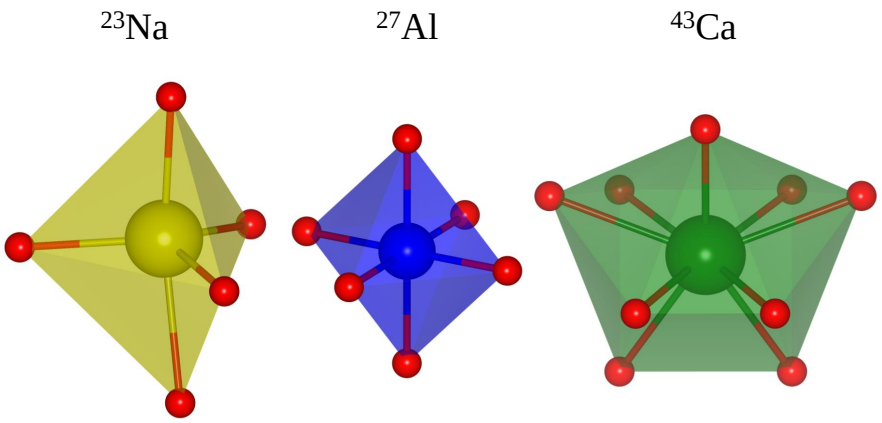

Figure 1. Oxygen coordination polyhedra for: fivefold-coordinated sodium in Na_2GeO_3 (ICSD no. 1622), sixfold-coordinated aluminum in $YAlO_3$ (ICSD no. 88261), and ninefold-coordinated calcium in $CaCO_3$ (aragonite, ICSD no. 32100).

Obviously, it would be advantageous if one could obtain information about the distances of oxygen coordination via the δ_{iso} parameter of the observed nuclide, which is comparatively easy to extract from NMR spectra. Such correlations have indeed been suggested for the oxygen coordination sphere of ^{23}Na [13,14], ^{27}Al [15], ^{43}Ca [16], and ^{207}Pb [17]. In these papers, it was assumed that the isotropic chemical shift of an observed nuclide X, which is surrounded only by oxygen, depends on the average X–O distance, d_{avg}, calculated over the oxygen atoms coordinating X. However, d_{avg} is distinctly dependent on the choice of this coordination sphere, and the coordination number (CN) defined by it. The question of how to define a coordination sphere in a periodic structure is indeed complex and still a matter of debate among chemists and crystallographers [18]. Recently, it has been suggested to circumvent this problem by using the shortest X–O distance found in the structure, d_{min}, instead of the average over the neighboring atoms. For ^{207}Pb (with spin $I = 1/2$) in oxygen surroundings, use of d_{min} leads to improvements in the correlation [19].

In the present work, we extend the concept of correlating δ_{iso} of the observed nuclide with its distance to the nearest oxygen to NMR spectroscopy of ^{23}Na ($I = 3/2$), ^{27}Al ($I = 5/2$), and ^{43}Ca ($I = 7/2$). For all three nuclei, it is shown that the quality of the correlations is similar to or better than those obtained by using d_{avg}, while removing the ambiguity inherent in the definition of the coordination sphere.

2. Materials and Methods

Isotropic chemical shift values δ_{iso} were collected from the literature, with the specific references listed in Tables A1–A3. It should be noted that all nuclides considered here have a spin $I > 1/2$ and thus possess a quadrupole moment [20]. For non-cubic electronic surroundings, this affects the NMR energy levels by the so-called quadrupole coupling, which is the interaction between the quadrupole moment of the nucleus and the electric field gradient (EFG) of the surroundings. For large coupling constants, the resonance position of the central transition is affected by it, in addition to the change of position caused by the chemical shift. This "quadrupolar shift" needs to be corrected for when

determining δ_{iso}. For the literature NMR results used in the current work, we only selected studies where (i) the quadrupolar shift was properly considered (whenever necessary), and (ii) the applied referencing for the chemical shift was clearly defined. The most common reference systems are: 1M NaCl solution for ^{23}Na, Al^{3+} in aqueous solution for ^{27}Al, and 1M $CaCl_2$ solution for ^{43}Ca. In some cases, when the relation of different reference material was well known, the originally reported δ_{iso} values were corrected to the references listed above. This meant adding 7.2 ppm when solid NaCl was used as reference for ^{23}Na [21], and adding 8 ppm when a saturated $CaCl_2$ solution was used [22]. (Theoretically, the change in Larmor frequency needs to be considered when moving a reference; however, for corrections <10 ppm, this makes practically no difference).

For those compounds selected on the grounds of rigorous and sound NMR characterization, the needed structural parameters were extracted from the Inorganic Crystal Structure Database (ICSD, provided by FIZ Karlsruhe GmbH). In case of multiple entries for one compound, the selection criteria were data quality, goodness of *R*-factor, the age of the publication, and the consistency with other structural models. To determine distances, the implemented ICSD function "Distances and Angles" was employed. The standard settings of this tool define the first coordination sphere by taking bond lengths in the range between 0.7 and 3.0 Å into account, which were accordingly used for our evaluations.

3. Results

3.1. NMR of ^{23}Na with $I = 3/2$ in Oxygen Coordination

The isotropic chemical shifts (δ_{iso}) of ^{23}Na in a number of inorganic compounds are tabulated in Table A1 in Appendix A, together with the parameters of their crystal structures: coordination numbers (*CN*), and both the average (d_{avg}) and minimal sodium–oxygen (d_{min}) distance within the coordination sphere. Figure 2a shows the plot of δ_{iso} versus d_{avg}, and Figure 2b the plot of δ_{iso} versus d_{min}. The data points in both plots display appreciable scatter, leading to Pearson correlation coefficients [23] that are comparatively low. By considering classes of sodium-containing compounds such as silicates, borates, carbonates, etc. in separate plots, these correlations can be substantially improved [14]. However, the purpose of the current work is to compare average to the shortest distance; therefore, members of various compound classes were included in our plots. It can be seen from the caption of Figure 2 that plotting the chemical shifts versus d_{min} leads to a marginally better correlation coefficient. While this improvement might not be significant, the important advantage of using the minimal distance to oxygen is that, in contrast to the average distance d_{avg}, it is unequivocally defined in the crystal structure.

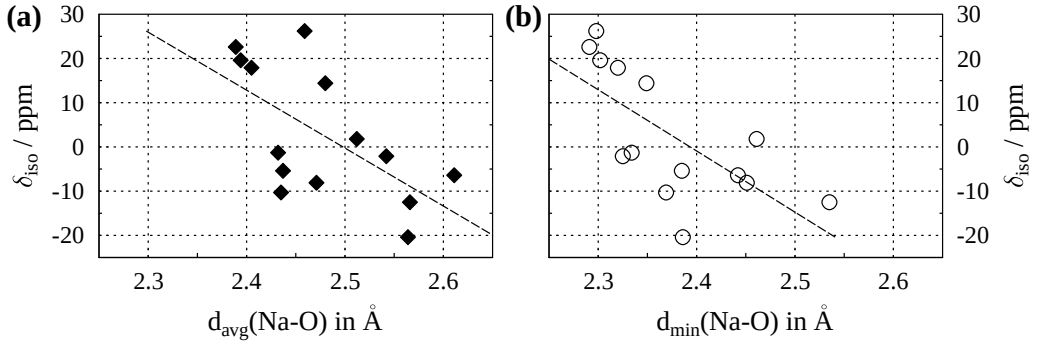

Figure 2. (**a**) Evolution of the ^{23}Na isotropic chemical shift (δ_{iso}) versus average Na–O distance, d_{avg}, for compounds where sodium is solely coordinated by oxygen. (**b**) δ_{iso} versus the shortest Na–O distance, d_{min}. Dashed lines show the least-square linear fits, which follow the relations $\delta_{iso} = (-131 \pm 48)d_{avg} + (328 \pm 119)$, with a Pearson correlation coefficient of $r_{avg} = 0.62$, and $\delta_{iso} = (-138 \pm 43)d_{min} + (330 \pm 103)$, with $r_{min} = 0.68$, respectively. All data are listed in Table A1.

3.2. NMR of ^{27}Al with $I = 5/2$ in Oxygen Coordination

The plots in Figure 3 show the ^{27}Al isotropic chemical shifts (δ_{iso}) versus average and shortest aluminum–oxygen distance in the crystal structures, with the relevant data listed in Table A2 in Appendix B. For the listed values of δ_{iso}, the absence of digits after the decimal points indicates that the estimated precision was ≥ 1 ppm. This may even apply for different crystallographic sites in a single compound, as may be seen from the entry for θ-Al_2O_3 in Table A2. Here, the site with the lower coordination number ($CN = 4$) experiences stronger quadrupole coupling (see also Section 2), which leads to broader lines and hence decreased the accuracy for determination of δ_{iso}. Regarding the scaling of the x-axis in Figure 3, it should be noted that for ^{27}Al, the interatomic distances to oxygen are significantly smaller than those reported for either ^{23}Na (see above) or ^{43}Ca (see below). This is due to the fact that Al^{3+} with its high net electrical charge has a larger atomic number than Na^+ despite both cations possessing an identical electron configuration. Compared to Na^+, and also to Ca^{2+} with its additional fully-occupied 3*s* and 3*p* orbitals, this leads to a smaller effective ionic radius for Al^{3+}. This effect is also visible in the graphics of Figure 1. An alternative view of the situation is to consider the role of covalency. Since the difference in electronegativity between oxygen and aluminum (≈1.8) is much lower than those of sodium (≈2.5) and calcium (≈2.4), a higher degree of covalent character is expected for aluminum–oxygen compounds. The more directed nature of covalent bonding leads to shorter distances.

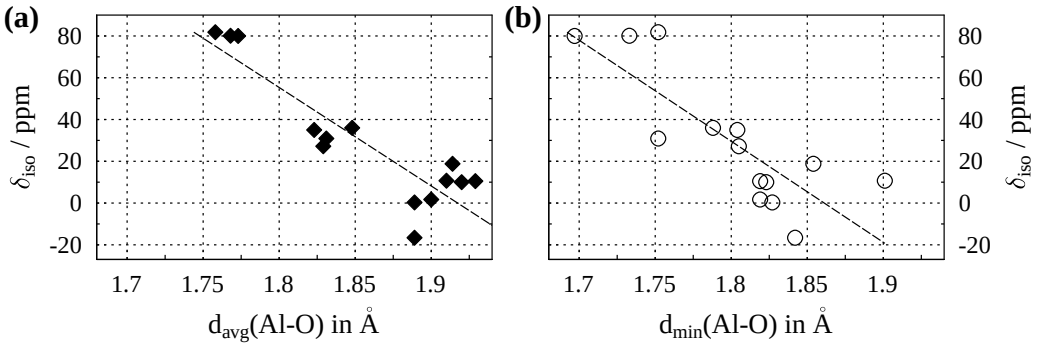

Figure 3. (**a**) Evolution of the ^{27}Al isotropic chemical shift (δ_{iso}) versus average Al–O distance, d_{avg}, for compounds where aluminum is solely coordinated by oxygen. (**b**) δ_{iso} versus the shortest Al–O distance, d_{min}. Dashed lines show the least-square linear fits, which follow the relations $\delta_{iso} = (-471 \pm 67)d_{avg} + (904 \pm 125)$, with a Pearson correlation coefficient of $r_{avg} = 0.90$, and $\delta_{iso} = (-484 \pm 99)d_{min} + (900 \pm 178)$, with $r_{min} = 0.82$, respectively. All data are listed in Table A2.

Figure 3a shows a remarkably strong clustering of the data points according to their coordination number (CN). The highest shift values are observed for the $CN = 4$, the lowest for $CN = 6$, with those for $CN = 5$ clearly separated in between. Apparently, this clustering also leads to correlation coefficients that are much better than those observed for the ^{23}Na data discussed above. One possible explanation for the clustering is to again consider the non-negligible covalent character in the bond interactions of aluminum discussed above. In a coordination sphere realized only by covalent bonds (i.e., a molecule), the number of coordination partners and the bond lengths are clearly defined. Thus, the presence of some covalent character in the aluminum compounds would narrow the spread of available distances and lead to the cluster effect observed in Figure 3a. For the plot of the minimal distances in Figure 3b, the clustering was less pronounced, with the data points for five- and sixfold-coordination overlapping. From the caption of Figure 3, it may be seen that for ^{27}Al, use of the shortest distances leads to a correlation coefficient that is slightly worse than that for use of d_{avg}. However, the resulting linear equations are very similar; and again, finding d_{min} in a given structure is much easier than defining average distances.

3.3. NMR of ^{43}Ca with $I = 7/2$ in Oxygen Coordination

Figure 4 shows δ_{iso} values of ^{43}Ca plotted versus average and shortest calcium–oxygen distance in the crystal structures, with the relevant data listed in Table A3 in Appendix C. In comparison to both ^{23}Na and ^{27}Al, the coordination number (CN) of ^{43}Ca is generally higher, with $CN \geq 7$. This is due to the larger size of the calcium ion (see also Figure 1), which allows for more neighbors in the coordination sphere. Some clustering according to the coordination number can be seen in Figure 4a. For ^{43}Ca, this only separates off the compounds with $CN = 12$, whereas the values for $CN = 7 \ldots 9$ all overlap; hence, the cluster effect is much weaker than that observed for ^{27}Al, cf. Figure 3a. From the data considered in this paper, the improvement in the correlation when using minimal instead of average distances to oxygen is the largest for ^{43}Ca (see also Figure 4b), with the Pearson correlation coefficient increasing from $r_{avg} = 0.43$ to $r_{min} = 0.70$. Similar to ^{27}Al, the clustering effect in the plots disappears when using d_{min} instead of d_{avg}.

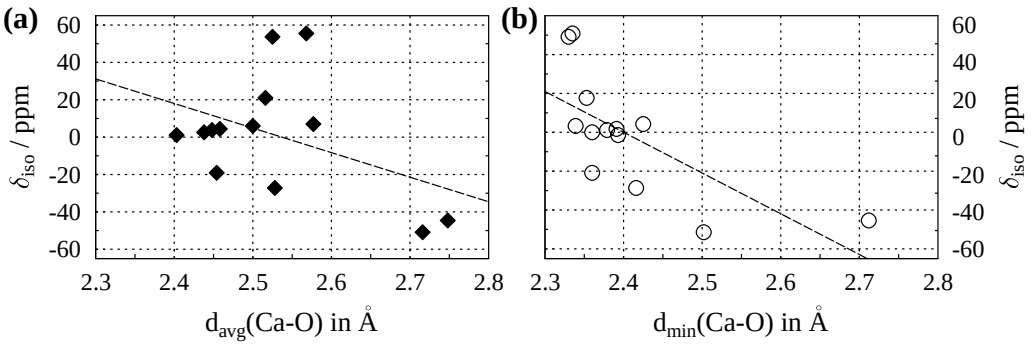

Figure 4. (**a**) Evolution of the ^{43}Ca isotropic chemical shift (δ_{iso}) versus average Ca–O distance, d_{avg}, for compounds where calcium is solely coordinated by oxygen. (**b**) δ_{iso} versus the shortest Ca–O distance, d_{min}. Dashed lines show the least-square linear fits, which follow the relations $\delta_{iso} = (-131 \pm 84)d_{avg} + (334 \pm 212)$, with a Pearson correlation coefficient of $r_{avg} = 0.43$, and $\delta_{iso} = (-218 \pm 66)d_{min} + (526 \pm 160)$, with $r_{min} = 0.70$, respectively. All data are listed in Table A3.

4. Discussion

In the context of relating NMR parameters to structural features in inorganic compounds, we investigated the relation of the isotropic chemical shift (δ_{iso}) of the nuclides ^{23}Na (with spin $I = 3/2$), ^{27}Al ($I = 5/2$), and ^{43}Ca ($I = 7/2$) in pure oxygen coordination to the nuclide–oxygen distances in their coordination sphere. It could be shown that the correlation of δ_{iso} with the shortest oxygen distance [19] works about as well as using the average oxygen distance [13–17] for ^{23}Na and ^{27}Al and even better for ^{43}Ca. Use of the minimal distance has the additional advantage that this parameter is uniquely defined. In contrast, the calculation of an average distance is strongly dependent on the definition of the oxygen coordination sphere, which may be contentious in some crystal structures.

Author Contributions: Conceptualization, O.E.O.Z. and T.B.; methodology, J.S., O.E.O.Z. and T.B.; formal analysis, J.S. and T.B.; writing—original draft preparation, J.S. and T.B.; writing—review and editing, J.S., O.E.O.Z. and T.B.; supervision, T.B. All authors have read and agreed to the published version of the manuscript.

Funding: This research received no external funding.

Institutional Review Board Statement: Not applicable.

Informed Consent Statement: Not applicable.

Data Availability Statement: The data are contained within the article.

Acknowledgments: J.S. and T.B. would like to thank Wolfgang Schnick (University of Munich, LMU) for continuing financial support.

Conflicts of Interest: The authors declare no conflict of interest.

Abbreviations

The following abbreviations are used in this manuscript:

CN	Coordination Number
ICSD	Inorganic Crystal Structure Database
MDPI	Multidisciplinary Digital Publishing Institute
NMR	Nuclear Magnetic Resonance
XRD	X-ray Diffraction

Appendix A. Chemical Shifts and Structural Parameters for ^{23}Na

Table A1. ^{23}Na isotropic chemical shifts δ_{iso} of compounds containing sodium in pure oxygen coordination. The shifts are reported relative (and where necessary, have been converted) to a 1M NaCl solution. Also listed are the coordination numbers (CN) of sodium and the distances to the surrounding oxygens in the crystal structure. The literature references refer to the NMR work and the crystallographic references may be traced to via their entry code in the ICSD.

Compound	ICSD Code (year)	Space Group (no.)	CN	d_{avg}/Å (Na–O)	d_{min}/Å (Na–O)	δ_{iso}/ppm	Ref.
$NaAlO_2$	14780 (2020)	$Pna2_1$ (33)	5	2.459	2.298	26.2	[24]
Na_2GeO_3	1622 (1978)	$Cmc2_1$ (36)	5	2.398	2.291	22.6	[14]
$Na_4B_2O_5$	10061 (1979)	$C2/c$ (15)	5	2.394	2.302	19.6	[14]
			6	2.480	2.349	14.4	
$Na_2C_2O_4$	56906 (1981)	$P2_1/c$ (14)	6	2.405	2.320	17.9	[25]
$NaBO_2$	34645 (1963)	$R\bar{3}c$ (167)	7	2.512	2.461	1.8	[14]
Na_2SO_4	28056 (1975)	$Fddd$ (70)	6	2.432	2.334	−1.3	[24]
$Na_4Ge_9O_{20}$	68507 (1990)	$I4_1/a$ (88)	6	2.542	2.325	−2.1	[14]
$NaHCO_3$	18183 (1965)	$P2_1/c$ (14)	6	2.437	2.385	−5.4	[26]
$Na_2Ge_4O_9$	189269 (2013)	$P\bar{3}c1$ (165)	7	2.611	2.442	−6.4	[14]
$NaNO_2$	68707 (1990)	$Im2m$ (44)	6	2.471	2.451	−8.1	[25]
β-$NaVO_3$	29450 (1984)	$Pnma$ (62)	6	2.435	2.369	−10.3	[25]
$NaIO_4$	14287 (1970)	$I4_1/a$ (88)	8	2.566	2.535	−12.5	[26]
$NaClO_4$	200405 (1978)	$Cmcm$ (63)	8	2.564	2.386	−20.4	[26]

Appendix B. Chemical Shifts and Structural Parameters for ^{27}Al

Table A2. ^{27}Al isotropic chemical shifts δ_{iso} of compounds containing aluminum in pure oxygen coordination. The shifts are reported relative to Al^{3+} in aqueous solution. Also listed are the coordination numbers (CN) of aluminum and the distances to the surrounding oxygens in the crystal structure. The literature references refer to the NMR work and the crystallographic references may be traced to via their entry code in the ICSD.

Compound	ICSD Code (year)	Space Group (no.)	CN	d_{avg}/Å (Al–O)	d_{min}/Å (Al–O)	δ_{iso}/ppm	Ref.
γ-$LiAlO_2$	430184 (2016)	$P4_12_12$ (92)	4	1.758	1.752	81.8	[27]
β-$NaAlO_2$	14780 (2020)	$Pna2_1$ (33)	4	1.768	1.733	80.1	[28]
θ-Al_2O_3	82504 (1996)	$C2/m$ (12)	4	1.773	1.697	80	[29]
			6	1.929	1.819	10.5	
$Al_2PO_4(OH)_3 \cdot H_2O$ (senegalite)	100542 (1979)	$P2_1nb$ (33)	5	1.848	1.788	36	[30]
			6	1.900	1.819	1.7	
Al_2SiO_5 (andalusite)	172728 (2006)	$Pnnm$ (58)	5	1.823	1.804	35	[31]
			6	1.920	1.823	10	
$Al_2PO_4(OH)_3$ (augelite)	426641 (2014)	$C2/m$ (12)	5	1.831	1.752	30.9	[30]
			6	1.889	1.827	0.3	
$AlVO_4$	55870 (2004)	$P\bar{1}$ (2)	5	1.829	1.805	27.2	[32]
α-Al_2O_3	51687 (2001)	$R\bar{3}c$ (167)	6	1.914	1.854	18.8	[33]
$YAlO_3$	88261 (1999)	$Pbnm$ (62)	6	1.910	1.901	10.7	[34]
$KAlP_2O_7$	2888 (1973)	$P2_1/c$ (14)	6	1.889	1.842	−16.6	[35]

Appendix C. Chemical Shifts and Structural Parameters for ^{43}Ca

Table A3. ^{43}Ca isotropic chemical shifts δ_{iso} of compounds containing calcium in pure oxygen coordination. The shifts are reported relative (and where necessary, have been converted) to a 1M $CaCl_2$ solution. Also listed are the coordination numbers (CN) of calcium and the distances to the surrounding oxygens in the crystal structure. The literature references refer to the NMR work and the crystallographic references may be traced to via their entry code in the ICSD.

Compound	ICSD Code (year)	Space Group (no.)	CN	d_{avg}/Å (Ca–O)	d_{min}/Å (Ca–O)	δ_{iso}/ppm	Ref.
$CaZrO_3$	97463 (2003)	*Pcmn* (62)	8	2.568	2.335	55.5	[36]
$CaAl_4O_7$	14270 (1970)	*C*2/*c* (15)	7	2.525	2.330	53.7	[37]
$CaTiO_3$	153172 (2005)	*Pbnm* (62)	8	2.516	2.353	21.0	[38]
$Ca_2MgSi_2O_7$	100736 (1981)	$P\bar{4}2_1m$ (113)	8	2.577	2.425	7	[39]
CaB_2O_4	62430 (1987)	*Pnca* (60)	8	2.500	2.339	6	[22]
$CaC_2O_4 \cdot 2H_2O$	30783 (1980)	*I*4/*m* (87)	8	2.458	2.391	4.4	[40]
$CaC_2O_4 \cdot 3H_2O$	159351 (1981)	$P\bar{1}$ (2)	8	2.448	2.379	3.8	[41]
$CaWO_4$	5510 (2019)	$I4_1/a$ (88)	8	2.438	2.360	2.6	[36]
$CaMoO_4$	60556 (1985)	$I4_1/a$ (88)	8	2.403	2.393	1.1	[36]
$CaSO_4 \cdot 2H_2O$	161622 (2008)	*C*2/*c* (15)	8	2.454	2.360	−19.1	[38]
$CaCO_3$ (aragonite)	32100 (1986)	*Pmcn* (62)	9	2.528	2.416	−27.2	[42]
$CaAl_{12}O_{19}$	202616 (1988)	$P6_3/mmc$ (194)	12	2.748	2.712	−44.6	[37]
$Ca(NO_3)_2$	52351 (1931)	$Pa\bar{3}$ (205)	12	2.716	2.502	−50.9	[38]

References

1. Bloch, F. Nuclear Induction. *Phys. Rev.* **1946**, *70*, 460–474. [CrossRef]
2. Abragam, A. *The Principles of Nuclear Magnetism*; Oxford University Press: Oxford, UK, 1961; ISBN 978-0-19-852014-6.
3. Ernst, R.R.; Bodenhausen, G.; Wokaun, A. *Principles of Nuclear Magnetic Resonance in One and Two Dimensions*; Clarendon Press: Oxford, UK, 1987; ISBN 0-19-855647-0.
4. MacKenzie, K.J.D.; Smith, M.E. *Multinuclear Solid-State NMR of Inorganic Materials*; Pergamon Materials Series v. 6; Pergamon: Oxford, UK, 2002; ISBN 0-08-043787-7.
5. Harris, R.K. NMR crystallography: The use of chemical shifts. *Solid State Sci.* **2004**, *6*, 1025–1037. [CrossRef]
6. Taulelle, F. NMR crystallography: Crystallochemical formula and space group selection. *Solid State Sci.* **2004**, *6*, 1053–1057. [CrossRef]
7. Bryce, D.L. NMR crystallography: Structure and properties of materials from solid-state nuclear magnetic resonance observables. *IUCrJ* **2017**, *4*, 350–359. [CrossRef]
8. Commission on NMR Crystallography and Related Methods. Available online: https://www.iucr.org/iucr/commissions/nmr-crystallography (accessed on 7 July 2022).
9. Andrew, E.R. Magic angle spinning in solid state n.m.r. spectroscopy. *Phil. Trans. R. Soc. A* **1981**, *299*, 505–520.

10. Herzfeld, J.; Berger, A.E. Sideband intensities in NMR spectra of samples spinning at the magic angle. *J. Chem. Phys.* **1980**, *73*, 6021–6030. [CrossRef]
11. Hodgkinson, P.; Emsley, L. The reliability of the determination of tensor parameters by solid-state nuclear magnetic resonance. *J. Chem. Phys.* **1997**, *107*, 4808–4816. [CrossRef]
12. Vosegaard, T. Single-crystal NMR spectroscopy. *Prog. Nucl. Magn. Reson. Spectr.* **2021**, *123*, 51–72. [CrossRef]
13. Xue, X.; Stebbins, J.F. ^{23}Na NMR chemical shifts and local Na coordination environments in silicate crystals, melts and glasses. *Phys. Chem. Miner.* **1993**, *20*, 297–307. [CrossRef]
14. George, A.M.; Sen, S.; Stebbins, J.F. ^{23}Na chemical shifts and local structure in crystalline, glassy, and molten sodium borates and germanates. *Solid State Nucl. Magn. Reson.* **1997**, *10*, 9–17. [CrossRef]
15. Haouas, M.; Taulelle, F.; Martineau, C. Recent advances in application of ^{27}Al NMR spectroscopy to materials science. *Prog. Nucl. Magn. Reson. Spectr.* **2016**, *94–95*, 11–36. [CrossRef] [PubMed]
16. Gambuzzi, E.; Pedone, A.; Menziani, M.C.; Angeli, F.; Florian, P.; Charpentier, T. Calcium environment in silicate and aluminosilicate glasses probed by ^{43}Ca MQMAS NMR experiments and MD-GIPAW calculations. *Solid State Nucl. Magn. Reson.* **2015**, *68–69*, 31–36. [CrossRef] [PubMed]
17. Fayon, F.; Farnan, I.; Bessada, C.; Coutures, J.; Massiot, D.; Coutures, J. P. Empirical Correlations between ^{207}Pb NMR Chemical Shifts and Structure in Solids. *J. Am. Chem. Soc.* **1997**, *119*, 6837–6843. [CrossRef]
18. Hoppe, R. Effective coordination numbers (ECoN) and mean Active ionic radii (MEFIR). *Z. Kristallog.-Cryst. Mater.* **1979**, *150*, 23–52. [CrossRef]
19. Zeman, O.E.O.; Steinadler, J.; Hochleitner, R.; Bräuniger, T. Determination of the Full ^{207}Pb Chemical Shift Tensor of Anglesite, $PbSO_4$, and Correlation of the Isotropic Shift to Lead-Oxygen Distance in Natural Minerals. *Crystals* **2019**, *9*, 43. [CrossRef]
20. Cohen, M.H.; Reif, F. Quadrupole effects in nuclear magnetic resonance studies of solids. *Solid State Phys.* **1957**, *5*, 321–438. [CrossRef]
21. Engelhardt, G.; Koller, H. A simple procedure for the determination of the quadrupole interaction parameters and isotropic chemical shifts from magic angle spinning NMR spectra of half-integer spin nuclei in solids. *Magn. Reson. Chem.* **1991**, *29*, 941–945. [CrossRef]
22. Gervais, C.; Laurencin, D.; Wong, A.; Pourpoint, F.; Labram, J.; Woodward, B.; Howes, A.P.; Pike, K.J.; Dupree, R.; Mauri, F.; et al. New perspectives on calcium environments in inorganic materials containing calcium-oxygen bonds: A combined computational-experimental ^{43}Ca NMR approach. *Chem. Phys. Lett.* **2008**, *464*, 42–48. [CrossRef]
23. Pearson, K. Note on regression and inheritance in the case of two parents. *Proc. R. Soc. Lond.* **1895**, *58*, 240–242.
24. Koller, H.; Engelhardt, G.; Kentgens, A.P.M.; Sauer, J. ^{23}Na NMR spectroscopy of solids: Interpretation of quadrupole interaction parameters and chemical shifts. *J. Phys. Chem.* **1994**, *98*, 1544–1551. [CrossRef]
25. Skibsted, J.; Nielsen, N.C.; Bildsøe, H.; Jakobsen, H.J. Satellite transitions in MAS NMR spectra of quadrupolar nuclei. *J. Magn. Reson.* **1991**, *95*, 88–117. [CrossRef]
26. Tabeta, R.; Saito, H. ^{23}Na chemical shifts of some inorganic and organic compounds in the solid state as determined by the magic angle spinning and high power NMR methods. *Chem. Lett.* **1984**, *13*, 293–296. [CrossRef]
27. Bräuniger, T.; Groh, B.; Moudrakovski, I.L.; Indris, S. Local electronic structure in γ-$LiAlO_2$ studied by single-crystal ^{27}Al NMR and DFT calculations. *J. Phys. Chem. A* **2016**, *120*, 7839–7846. [CrossRef]
28. Müller, D.; Gessner, W.; Samoson, A.; Lippmaa, E.; Scheler, G. Solid-state aluminium-27 nuclear magnetic resonance chemical shift and quadrupole coupling data for condensed AlO_4 tetrahedra. *J. Chem. Soc. Dalton Trans.* **1986**, *6*, 1277–1281. [CrossRef]
29. O'Dell, L.A.; Savin, S.L.P.; Chadwick, A.V.; Smith, M.E. A ^{27}Al MAS NMR study of a sol-gel produced alumina: Identification of the NMR parameters of the θ-Al_2O_3 transition alumina phase. *Solid State Nucl. Magn. Reson.* **2007**, *31*, 169–173. [CrossRef] [PubMed]
30. Bleam, W.F.; Dec, S.F.; Frye, J.S. ^{27}Al Solid-state Nuclear Magnetic Resonance Study of Five-Coordinate Aluminum in Augelite and Senegalite. *Phys. Chem. Miner.* **1989**, *16*, 817–820. [CrossRef]
31. Alemany, L.B.; Massiot, D.; Sherriff, B.L.; Smith, M.E.; Taulelle, F. Observation and accurate quantification of ^{27}Al MAS NMR spectra of some Al_2SiO_5 polymorphs containing sites with large quadrupole interactions. *Chem. Phys. Lett.* **1991**, *177*, 301–306. [CrossRef]
32. Nielsen, U.G.; Boisen, A.; Brorson, M.; Jacobsen, C.J.H.; Jakobsen, H.J.; Skibsted, J. Aluminum orthovanadate ($AlVO_4$): Synthesis and characterization by ^{27}Al and ^{51}V MAS and MQMAS NMR spectroscopy. *Inorg. Chem.* **2002**, *41*, 6432–6439. [CrossRef]
33. Vosegaard, T.; Jakobsen, H.J. ^{27}Al Chemical Shielding Anisotropy. *J. Magn. Reson.* **1997**, *128*, 135–137. jmre.1997.1236. [CrossRef]
34. Florian, P.; Gervais, M.; Douy, A.; Massiot, D.; Coutures, J.-P. A Multi-nuclear Multiple-Field Nuclear Magnetic Resonance Study of the Y_2O_3—Al_2O_3 Phase Diagram. *J. Phys. Chem. B* **2001**, *105*, 379–391. [CrossRef]
35. Müller, D.; Grunze, I.; Hallas, E.; Ladwig, G. Hochfeld-^{27}Al-NMR-Untersuchungen zur Aluminiumkoordination in kristallinen Aluminiumphosphaten. *Z. Anorg. Allg. Chem.* **1983**, *500*, 80–88. [CrossRef]
36. Lin, Z.; Smith, M.E.; Sowrey, F.E.; Newport, R.J. Probing the local structural environment of calcium by natural-abundance solid-state ^{43}Ca NMR. *Phys. Rev. B* **2004**, *69*, 224107. [CrossRef]
37. MacKenzie, K.J.D.; Schmücker, M.; Smith, M.E.; Poplett, I.J.F.; Kemmitt, T. Evolution of crystalline aluminates from hybrid gel-derived precursors studied by XRD and multinuclear solid state MAS NMR IV: Calcium dialuminate, $CaAl_4O_7$ and calcium hexaaluminate, $CaAl_{12}O_{19}$. *Thermochim. Acta* **2000**, *363*, 181–188. [CrossRef]

38. Widdifield, C.M.; Moudrakovski, I.; Bryce, D.L. Calcium-43 chemical shift and electric field gradient tensor interplay: A sensitive probe of structure, polymorphism, and hydration. *Phys. Chem. Chem. Phys.* **2014**, *16*, 13340–13359. [CrossRef]
39. Dupree, R.; Howes, A.P.; Kohn, S.C. Natural abundance solid state ^{43}Ca NMR. *Chem. Phys. Lett.* **1997**, *276*, 399–404. [CrossRef]
40. Bowers, G.M.; Kirkpatrick, R.J. Natural Abundance ^{43}Ca NMR as a Tool for Exploring Calcium Biomineralization: Renal Stone Formation and Growth. *Cryst. Growth Des.* **2011**, *11*, 5188–5191. [CrossRef]
41. Wong, A.; Howes, A.P.; Dupree, R.; Smith, M.E. Natural abundance ^{43}Ca NMR study of calcium-containing organic solids: A model study for Ca-binding biomaterials. *Chem. Phys. Lett.* **2006**, *427*, 201–205. [CrossRef]
42. Huang, Y.-C.; Mou, Y.; Tsai, T.W.-T.; Wu, Y.-J.; Lee, H.-K.; Huang, S.-J.; Chan, J.C.C. Calcium-43 NMR Studies of Polymorphic Transition of Calcite to Aragonite. *J. Phys. Chem. B* **2012**, *116*, 14295–14301. [CrossRef]